Critical Role of Specific Ions for Ligand-Induced Changes Regulating Pyruvate Dehydrogenase Kinase Isoform 2†

Yasuaki Hiromasa and Thomas E. Roche*

Department of Biochemistry, Kansas State University, Manhattan, Kansas 66506

Received July 25, 2007; Revised Manuscript Received December 18, 2007

ABSTRACT: In the complete absence of K^+ and phosphate (P_i), pyruvate dehydrogenase kinase isoform 2 (PDHK2) was catalytically very active but with an elevated K_m for ATP, and this activity is insensitive to effector regulation. We find that K^+ or 5-fold lower levels of NH_4^+ markedly enhanced quenching of Trp383 fluorescence of PDHK2 by ADP and ATP. K^+ binding caused an ∼40-fold decrease in the equilibrium dissociation constants (K_d) for ATP from ∼120 to 3.0 μM and an ∼25-fold decrease in K_d for ADP from ∼950 to 38 μM. Linked reductions in K_d of PDHK2 for K^+ were from ∼30 to ∼0.75 mM with ATP bound and from ∼40 to ∼1.7 mM with ADP bound. Without K^+, there was little effect of ADP on pyruvate binding, but with 100 mM K^+ and 100 μM ADP, the $L_{0.5}$ of PDHK2 for pyruvate was reduced by ∼14 fold. In the absence of K^+, P_i had small effects on ligand binding. With 100 mM K^+, 20 mM P_i modestly enhanced binding of ADP and hindered pyruvate binding but markedly enhanced the binding of pyruvate with ADP; the $L_{0.5}$ for pyruvate was specifically decreased ∼125-fold with 100 μM ADP. P_i effects were minimal when NH_4^+ replaced K^+. We have quantified coupled binding of K^+ with ATP and ADP and elucidated how linked K^+ and P_i binding are required for the potent inhibition of PDHK2 by ADP and pyruvate.

The pyruvate dehydrogenase complex (PDC)[1] has a critical role in restraining the consumption of carbohydrate (*1*−*4*). Passage of pyruvate carbons through this reaction leads to the depletion of body carbohydrate reserves in mammals. To conserve carbohydrate, PDC activity is reduced by phosphorylation by the pyruvate dehydrogenase kinase (PDHK). There are four PDHK isozymes (PDHK1, PDHK2, PDHK3, and PDHK4) (*3*−*6*). PDHK2 is nearly universally distributed among tissues (*7*, *8*) and is particularly sensitive to signals indicating changes in fuel supply and energy demand (*8*−*13*). Use of fatty acids and ketone bodies is registered via increases in the NADH to NAD^+ and acetyl-CoA to CoA ratios fostering enhanced PDHK2 inactivation of PDC (*3*, *4*, *8*−*10*, *12*). A sufficient supply of carbohydrate is recognized via adequate pyruvate levels and the need for energy by a reduction in phosphate potential [ATP/ADP + phosphate (P_i)] (*3*, *4*, *11*, *13*). The combination of ADP and pyruvate potently inhibits PDHK2 activity (*8*, *9*, *11*). Because activation of PDC is an important target in medical conditions, such as heart ischemia and insulin resistant diabetes, PDHKs have been a target for development of specific inhibitors ranging from the early use of dichloroacetate (DCA) as a pyruvate analogue to development of the potent binding 3,3,3-trifluoro-2-hydroxy-2-methylpropanoyl-containing inhibitors, such as Nov3r, AZD7545, and compound K (*14*−*17*). These inhibitors potently inhibit PDHK2 (*17*) and have been shown to lower blood glucose levels in Zucker diabetic fatty rats (*18*, *19*).

Efficient catalysis by PDHK2 and stimulation by elevated levels of NADH and acetyl-CoA require binding of PDHK2 to the inner lipoyl domain (L2) of the dihydrolipoyl acetyltransferase (E2) component (*9*, *12*, *20*, *21*). Stimulation by elevated NADH and acetyl-CoA levels is mediated by reduction and acetylation of the lipoyl group of L2 via the reverse of the reactions catalyzed by dihydrolipoyl dehydrogenase (E3) and E2 components. Nov3r and related compounds bind at the lipoyl group binding site of PDHK2 (*22*) and hinder binding of PDHK2 to E2.[2]

Crystal structures of PDHK2 and PDHK3 dimers provide insights into the nature of the sites for binding ATP/ADP, pyruvate (DCA), the L2 domain, and the lipoyl group (Nov3r) (*22*−*24*). As shown in Figure 1, the ATP (ADP) binding site is in the catalytic (Cat) domain (residues 178−366) (*23*) and the DCA (pyruvate) and Nov3r (lipoyl group) binding sites are in the regulatory domain (residues 6−169)

† This work was supported by National Institutes of Health Grant DK18320, the American Heart Association, and the Agricultural Experiment Station (Contribution 08-30-J).

* To whom correspondence should be addressed: Department of Biochemistry, Chalmers Hall, Kansas State University, Manhattan, KS 66506. Phone: (785) 532-6116. Fax: (785) 532-7278. E-mail: bchter@ksu.edu.

[1] Abbreviations: PDC, pyruvate dehydrogenase complex; E1, pyruvate dehydrogenase component; E2, dihydrolipoyl acetyltransferase component; L1 domain, NH_2-terminal lipoyl domain of E2; L2 domain, interior lipoyl domain of E2; E3, dihydrolipoyl dehydrogenase component; E3BP, E3-binding protein; PDHK, pyruvate dehydrogenase kinase; GST, glutathione *S*-transferase; DCA, dichloroacetate; AUC, analytical ultracentrifugation; $L_{0.5}$, ligand concentration giving half-maximal quenching; Q_{obs}, Q_{max}, and Q_{tot}, observed, maximal, and total quenching, respectively; *n*, Hill coefficient; *C*, coupling constant.

[2] Companion paper: Hiromasa, Y., Yan, X., and Roche, T. E. (2008) Specific Ion Influences on Self-Association of Pyruvate Dehydrogenase Kinase Isoform 2 (PDHK2), Binding of PDHK2 to the L2 Lipoyl Domain, and Effects of the Lipoyl Group-Binding Site Inhibitor, Nov3r, *Biochemistry 47,* 2312−2324.

10.1021/bi701475f CCC: $40.75
Published on Web 01/26/2008

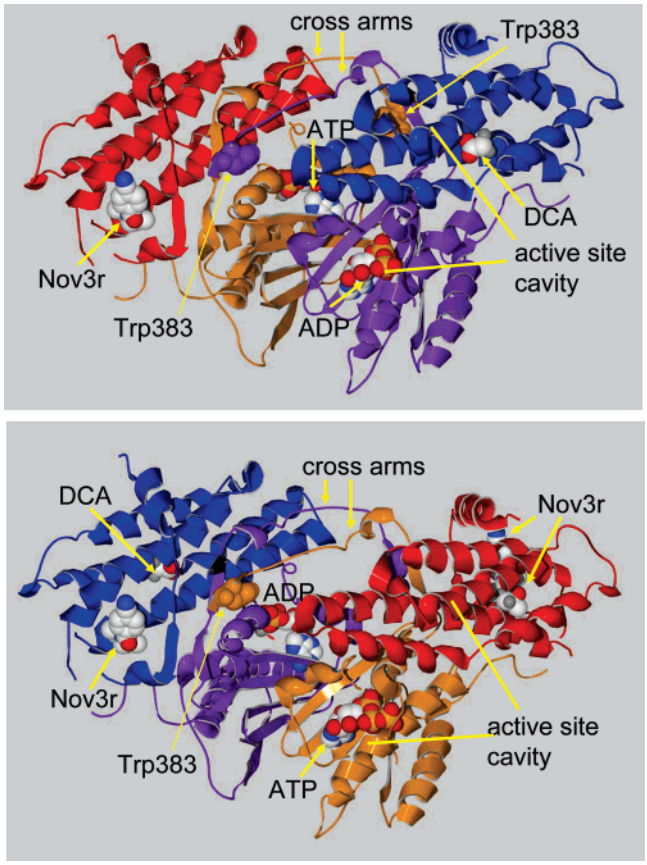

FIGURE 1: PDHK2 dimer structure. Viewed from opposite sides in the two views, ribbon structures are shown for the backbone of the subunits of the PDHK2 dimer. One subunit of the dimer has an orange Cat domain that binds ATP at the active site and a red R domain that binds Nov3r at the lipoyl group binding site. The other subunit has a violet Cat domain holding ADP at the active site and a blue R domain with the R domain that binds DCA in both views and also Nov3r in the bottom view. Intersubunit cross arms are also shown with Trp383 residues (space-filled) which play a key role in anchoring the intersubunit cross arms via an interaction between the R and Cat domains of the other subunit (*22*). The figures were prepared using the DeepView program; all protein structure was from the PDHK2 dimer structure binding ATP and Nov3r (PDB entry 2bu2) (*22*). The PDHK2 monomer with ADP and DCA bound (PDB entry 2bu8) (*22*) was aligned with one of the subunits of the dimer; this PDB entry was used only for introducing ADP and DCA. The backbones of PDHK2 from these two PDB entries are tightly superimposed so that the locations of bound ligands are presented accurately.

(*22*, *24*). The ATP/ADP binding site in the Cat domain is located at one end of an extended interface between the R and Cat domains at each end of the PDHK2 dimer. In the middle of the large active site cavity, the binding of DCA shows the location of the pyruvate binding site in the R domain in a position just above the Cat domain−R domain interface (Figure 1) (*22*). Opposite this outward-facing cavity, the Cat domains of each subunit associate, and rising from this base, the R domains frame a large trough opening. In some PDHK2 structures, C-terminal cross arms (residues 366−383) span this trough region between subunits (Figure 1) (*22*). On the basis of the PDHK3·L2 complex, a combination of this intersubunit cross arm and most of the remaining part of the C-terminus (residues 383−405) combine with the trough side of the R domain to bind the L2 domain of E2 (Figure 1 of the companion paper[2]) (*24*). The lipoyl group of L2 (*24*) or Nov3r (Figure 1) (*22*) binds in a deep, narrow cleft on this trough side of the R domain.

Prior studies indicate that the K_m of PDHK for ATP is decreased by including K^+ ion (*11*, *25*), that effective stimulation of PDHK increases when kinase activity is restrained by elevating ion levels (especially K^+ and P_i) (*11*, *26*), and that K^+-aided binding of ADP favors pyruvate inhibition (*11*, *27*). Detailed kinetic and other studies on PDHK2 indicate that, using buffers with near-physiological levels of K^+ (100−130 mM), dissociation of ADP limits PDHK2 activity and that reductive acetylation of E2 accelerates dissociation of ADP from PDHK2 (*11*, *12*). Crystal structures revealed K^+ binding at the entrance to the active site of the related branched chain dehydrogenase kinase (BCDK) (*28*) and the PDHK3 isoform (*24*) with an oxygen of the α-phosphate of bound ATP or ADP contributing to K^+ binding. Similar binding was readily modeled in PDHK2 structures (*22*). These findings suggest that enforcing or removing trapdoor binding of K^+ after ATP or ADP binding[3] may play a critical role in regulating PDHK2 activity. We provide direct quantitative evidence that supports the hypothesis of K^+ slowing ADP dissociation and also reveal a major K^+-dependent role of P_i in supporting coupled binding of ADP and pyruvate. The companion paper[2] provides evidence consistent with weakened binding of K^+/ADP at the active site due to binding at the lipoyl binding site; moreover, P_i has important intervening roles in transmitting this effect as well as in ADP with pyruvate interfering with lipoyl domain binding and causing PDHK2 to form a tetramer.

We have recently found that binding of ATP, ADP, or pyruvate induces substantial conformational changes in PDHK2 as reported by Trp fluorescence quenching, primarily involving Trp383 (*13*). In the trough region, Trp383 is located at the end of each trough-spanning intersubunit cross arm (Figure 1), well away from ligand binding sites (*13*, *22*). Each Trp383 is wedged into the surface of the other subunit at the trough−side interface between the Cat and R domains. Using potassium phosphate buffer, we found that the $L_{0.5}$ for pyruvate was reduced 150-fold via the introduction of ADP (*13*). Here, Trp fluorescence quenching is used to quantify the coupled binding of ATP, ADP, and K^+ and to demonstrate the essential roles of K^+ and P_i for high-affinity binding of pyruvate with ADP.

EXPERIMENTAL PROCEDURES

Materials. Using human PDC components, PDHK2 (*9*), E1 (*11*), and E2 [Supporting Information (*29*)] were prepared by recombinant techniques as previously described. To prepare PDHK2 in the absence of monovalent metals, PDHK2 was exhaustively dialyzed against or gel filtered into 20 mM Hepes-Tris buffer (pH 7.5) containing 0.5 mM EDTA. For some experiments, the buffer was changed further (e.g., EDTA removed) by further dialysis or gel filtration.

Fluorescence Quenching. Steady state fluorescence spectra were recorded with a Cary Eclipse fluorescence spectropho-

[3] ATP appears to dissociate slower than ADP, but that does not limit catalysis which appears to proceed by an ordered mechanism with ATP binding first (*11*, *12*). Capture of ATP by coupled binding of K^+ likely contributes to the observed findings. With such an ordered mechanism, the K_m for ATP is independent of rate constant for dissociation of ATP and dependent on the rate constant for dissociation of ADP (*11*).

tometer (Varian, Inc.) at 20 °C (*13*). Studies were conducted with 20 mM Hepes-Tris buffer (pH 7.5) normally containing 0.5 mM EDTA and 2.0 mM $MgCl_2$. The $MgCl_2$ level was increased when high levels of ATP or ADP were used. When K^+, NH_4^+, or Na^+ was added, Hepes was used as the counterion, and when P_i was added, Tris was used as the counterion. The levels of counterions in concentrates were adjusted such that a pH of 7.5 was obtained when the ion being varied was diluted to 50 mM. Throughout, the total ammonium concentration is reported as NH_4^+; however, ~1.75% is present as the neutral species at pH 7.5. Other conditions for obtaining steady state fluorescence spectra were as described previously (*13*). Using an initial level of 0.54 μM PDHK2 (0.050 A_{280}) in 2 mL, excitation was at 290−310 nm; higher wavelengths were used for excitation when adenine nucleotide levels were elevated. Fluorescence spectra were recorded from 320 to 420 nm using a standard quartz (1 cm × 1 cm) cuvette. Varied ligands were added in 2−10 μL increments; data analysis included continuously correcting the concentration of PDHK2 for the slight dilution due to these additions. The change in fluorescence at 350 nm was used to assess fluorescence quenching. The data were fit and standard deviations determined using either Sigma Plot or Origin (*13*) using the Hill equation:

$$Q_{obs} = (Q_{max}[A]^n)/(L_{0.5}{}^n + [A]^n) \quad (1)$$

where Q_{obs} is the observed quenching, n is the Hill coefficient, Q_{max} is the extrapolated maximal quenching (corrected in the fit for Q_{min}), and $L_{0.5}$ is the concentration giving half-maximal quenching.

ATP and ADP bound to Mg^{2+} are the primary species being bound and causing fluorescent quenching. Under different buffer conditions, the levels of ATP·Mg^{2-}, ATP·Mg^-, ATP·K^{3-}, free ATP^{4-} and ATP^{3-}, ADP·Mg^-, ADP·K^{2-}, free ADP^{3-} and ADP^{2-}, free Mg^{2+}, and Mg·HPO_4 were evaluated using the stability constants and pK_a values previously reported (*30*). Without K^+ or P_i, a direct algebraic solution was possible. With those ions, the calculations involved repeated calculation cycles as previously employed in estimating the level of free Ca^{2+} when based on added EGTA, EDTA, and Mg^{2+} at a given pH using the appropriate stability constants and pK_a values (*31*−*33*). Under our standard conditions of addition of 2 mM $MgCl_2$ and 0.5 mM EDTA at pH 7.5 and even with 100 mM K^+, >97% ATP is complexed to Mg^{2+} for ATP levels of <0.2 mM (e.g., with 100 μM ATP and 100 mM K^+, ~97.5% ATP·$Mg^{2-/-}$, ~1.5% ATP·K^{3-}, and ~1% free ATP). Because of the small error involved, plots of ATP concentration and parameters derived are based on total ATP concentrations. Prior to the addition of the varied ligand, free Mg^{2+} was normally 1.5 mM; higher levels were normally not used because $MgCl_2$ also modestly quenched (Supporting Information). However, as ATP or ADP levels exceeded 0.5 mM, higher levels of $MgCl_2$ were used. With just Mg^{2+} and ADP, we plot the ADP·Mg^- level in our evaluation of quenching with an increasing ADP level (Supporting Information). However, for ease in comparisons to prior results obtained with potassium phosphate buffer (*13*) and results with NH_4^+ for which we could not obtain a trustworthy stability constant for ADP·NH_4^{2-}, we show results with elevated K^+ levels (Figure 3 and 4B) based on the total ADP concentration. Nevertheless, data were analyzed for variation in quenching with the ADP·Mg^- level; $L_{0.5}$ values are reported for both ADP and ADP·Mg^- from studies with 100 mM K^+ (Table 3). The analysis of coupling with K^+ (procedures below) uses the $L_{0.5}$ values determined for ADP·Mg^-.

Data Fitting and Linkage Analysis for Two Ligands (ternary complex formation). The degree of allosteric coupling in the binding of two ligands can be quantified in terms of the coupling constant, $\check{C} = K_{iA}{}^0/K_{iA}{}^b = K_{iB}{}^0/K_{iB}{}^a$, the ratio of the equilibrium dissociation constant (use K_d in specific cases) in the absence of the second ligand over the equilibrium dissociation constant at a saturating concentration of the second ligand (*34*, *35*). Equality of those ratios derives from the relation $K_{iA}{}^0K_{iB}{}^a = K_{iB}{}^0K_{iA}{}^b$ based on the principles of microscopic reversibility which requires EAB to be an equivalent state whether created with A or B binding first. Therefore, the coupling constant, $\check{C}$, is a quantitative measure of the mutual effect that each of these ligands has on the change in the binding affinity of the other ligand; the coupling free energy $\ln \Delta G = RT \ln(\check{C})$. In theory, $\check{C}$ can be directly calculated from the binding K_d estimated in the absence of the saturating presence of the second ligand. In practice, the full set of K_d values for A and B is often not directly obtainable (e.g., when binding of a ligand by itself cannot be observed or when extrapolation is needed to evaluate the change at saturating levels of one of the ligands).

For linkage analysis with two ligands forming a ternary complex, we use two approaches. The first assumes random equilibrium binding. For two ligands A and B, data were fit using GOSA to random equilibrium eq 2

$$Q_{obs}/Q_{max}{}^{ab} = [(cK_{iB}{}^a)/B + (dK_{iA}{}^b)/A + 1]/[(K_{iA}{}^0K_{iB}{}^a)/(AB) + K_{iB}{}^a/B + K_{iA}{}^b/A + 1] \quad (2)$$

in which c and d are the fraction of maximum fluorescence quenching by EA and EB, respectively, over the maximum quenching ($Q_{max}{}^{ab}$) by EAB. Thus, this approach allowed us to account for different levels of quenching to fit data in which either ligand was varied at different fixed levels of the other ligand. In our studies, a typical case is one in which K_{iA}, Q_{max} for EAB, and $c = Q_{max}{}^a/Q_{max}{}^{ab}$ (and, if needed, $d = Q_{max}{}^b/Q_{max}{}^{ab}$) have been determined and $K_{iB}{}^a$ and $K_{iA}{}^b$ are fit. In the assessment of the statistical output, optimization was based on minimizing the sum of squared errors, the standard deviations in parameter fits, and maximizing the global correlation coefficient in that order of priority. The remaining equilibrium constant ($K_{iB}{}^0$ in the form of parameters in eq 2) is then calculated from the equations given above for microscopic reversibility or from the estimate derived for $\check{C}$. This approach assumes noncooperative (hyperbolic) binding of ligands which was not met in the case of the ATP level being varied at higher K^+ levels. Therefore, the data were also fit by the approach of Reinhart (*34*, *35*). When, for instance, $L_{0.5}$ values for ligand A have been determined from varying the A concentration at a series of different fixed levels of B using eq 1, the data are then fit by eq 3:

$$L_{0.5A} = K_{iA}{}^0(K_{iB}{}^0 + [B])/(K_{iB}{}^0 + \check{C}[B]) \quad (3)$$

The data are presented in a plot of $\log(L_{0.5A})$ on the y-axis for varied ligand levels versus log[B] on the x-axis for the

different concentrations of the fixed ligands. The measured and extrapolated fits at $B = 0$ and at saturating B yield log(K_{iA}^0) and log(K_{iA}^b), respectively, which are observed as plateau regions on the y-axis in the log−log plot. $\check{C}$ is estimated from the maximal change: log(K_{iA}^0) − log(K_{iA}^a) = log($\check{C}$). When separate data analysis gives K_{iB}^a (or $S_{0.5}$ for saturating A levels with $1 \ll n \gg 1$), this can be imposed on the above fit using $\check{C}K_{iB}^a$ for K_{iB}^0. This fit has an advantage in that it deals with cooperative responses as a ligand is varied, but it fails to deal with partial fluorescence quenching in forming EA or EB relative to the quenching by EAB. We note that since pH was not varied that estimates of $\check{C}$ and dissociation constants are conditional since the proton concentration probably affects these values. Large ligand effects demonstrating coupling are described for higher-order complexes (quaternary, etc.) that clearly involve multiple linkages in the binding of these ligands.

PDHK2 Activity Assays. PDHK2 activity assays were conducted using methods previously described (*9*, *11*). In short, PDHK activity was measured in duplicate or triplicate as the initial rate of incorporation of [^{32}P]phosphate into E1 using the indicated level of [γ-^{32}P]ATP (150−500 cpm/pmol) at 30 °C. PDHK2 assays, conducted with E2, routinely used 0.1−0.15 μg of PDHK2, 10 μg of E2, and 10−14 μg of E1 in a final volume of 25 μL. The enzyme components were preincubated at 4 °C for 1 h as a concentrate with 0.2 mM dithiothreitol, and aliquots were diluted at least 3-fold in the final assay mixture. Studies were conducted using the same buffer systems that were used in fluorescence studies. Average rates from assays, performed at least in duplicate, are reported. Assays for one condition were performed in duplicate at the beginning and end of a set of assays to evaluate enzyme stability. Repetitions or closely related experiments gave results that agreed within experimental error with the reported results.

RESULTS

As indicated in the introductory section, there is considerable evidence for K^+ contributing to mechanisms affecting the function and regulation of PDHK (*25*−*27*, *36*), including PDHK2 (*9*, *11*, *12*). However, neither the affinity of a kinase isoform for K^+ nor the quantitative effects of ligands on K^+ binding or the reciprocal effects of K^+ on ligand binding to a PDHK have been described. Structural studies are consistent with ATP/ADP-dependent binding of K^+ at the active site involving strong coordination to an oxygen of the α-phosphate of ATP/ADP (*22*, *24*). This proposed coordination and the location of the K^+ binding site toward the exterior of the ATP/ADP site suggest that binding of K^+ will occur with either ATP or ADP. In prior studies conducted using 50 mM potassium phosphate buffer (pH 7.5), ATP, ADP, pyruvate, and synergistically ADP in combination with pyruvate led to both marked quenching of Trp fluorescence of PDHK2 and a reduced level of binding of PDHK2 to the L2 domain of the E2 component (*13*). Here, we present evidence that specific ions (K^+ and P_i) directly contribute to the allosteric coupling to produce the large change in ligand binding that results in the "synergistic" inhibition of PDHK2 activity. We have used NH_4^+ as an effective analogue of K^+ ion; via these studies and those in the companion paper,[2] we have obtained evidence using NH_4^+ for variation in K^+ action. We also uncover weaker

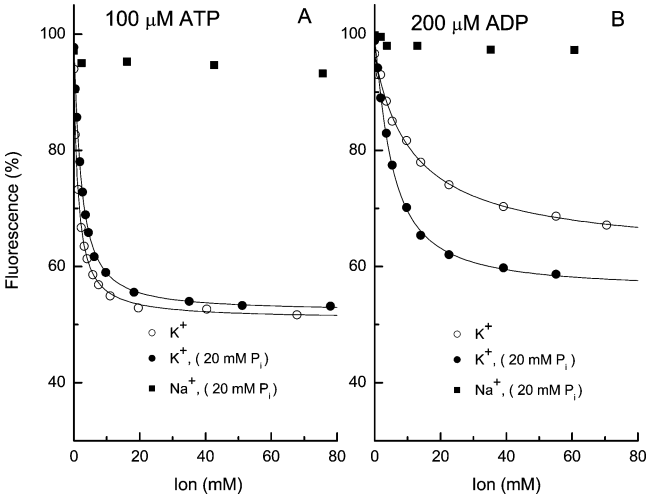

FIGURE 2: Dependence on K^+ concentration of quenching of Trp fluorescence by ATP or ADP in the absence or presence of 20 mM P_i. Fluorescence was measured at 350 nm as described in Experimental Procedures with 1.5 mM Mg^{2+} (beyond EDTA) and 100 μM ATP (A) or 200 μM ADP (B). Data with 20 mM P_i with Na^+ replacing K^+ as the varied ligand are also shown. The quenching profiles with K^+ were fit using eq 1.

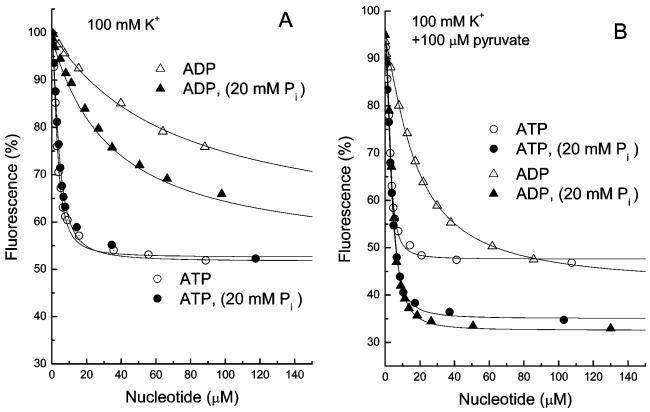

FIGURE 3: Quenching of Trp fluorescence by ADP and ATP in the presence of 100 mM K^+ and effects of addition of 20 mM P_i (A and B) and 100 μM pyruvate (B). Measurements were taken as described in the legend of Figure 2 and in Experimental Procedures. When the ADP level was varied, the change in quenching was also analyzed with the change in ADP·Mg^- (calculated as described in Experimental Procedures) with those $L_{0.5}$ values also reported in Table 3. Data points were collected with concentrations of ADP of up to ~310 μM.

fluorescence quenching by ATP and ADP alone (Supporting Information) that allowed us to carry out limited linkage analyses of the coupling in ATP or ADP binding with K^+. We show the linkage between pyruvate and ADP requires K^+ and is enhanced by P_i. The companion paper[2] establishes critical roles of P_i in other interactions.

K^+ Requirement for Strong Quenching of Trp383 Fluorescence of PDHK2. In potassium phosphate buffer, fluorescence quenching of PDHK2 by ATP or ADP was completely removed with the W383F-PDHK2 mutant (*13*). By themselves, increasing levels of K^+ or Na^+ up to 100 mM gave <1% quenching of Trp fluorescence and 50 mM NH_4^+ gave ≤3% quenching; even with 100 mM K^+, 20 mM P_i caused ≤3% quenching (Figure 1SA, Supporting Information). With initially 1.5 mM free Mg^{2+}, Figure 2 shows that increasing the K^+ level greatly enhances fluorescence quenching with 100 μM ATP (>97.5 μM ATP·$Mg^{2-/-}$ and

Table 1: K^+ and NH_4^+ Ion Concentration Dependence for Quenching of Trp Fluorescence of PDHK2[a]

	K^+ varied			NH_4^+ varied	
fixed ligand(s)	$L_{0.5}$[b] (mM)	Q_{max}[c] (%)	Q_{tot}[d] (%)	$L_{0.5}$[b] (mM)	Q_{max}[c] (%)
5 μM ATP	11 ± 2	42.0 ± 1.5	~42.5		
50 μM ATP	2.1 ± 0.3	40.5 ± 1.3	~43.5		
100 μM ATP	1.33 ± 0.5	43.0 ± 0.35	~47.0	0.26 ± 0.01	46.0 ± 0.2
1000 μM ATP	0.84 ± 0.06	36.0 ± 1.0	~49.0		
100 μM ATP, 20 mM P_i	2.20 ± 0.07	43.3 ± 0.3	~48.5	0.37 ± 0.07	46 ± 2
50 μM ADP	20.5 ± 4	24 ± 2.5	~25		
200 μM ADP	12 ± 1.5	34.5 ± 2.0	~37	2.8 ± 0.15	38.0 ± 0.5
200 μM ADP, 20 mM P_i	5.3 ± 0.2	43 ± 1	~45	2.4 ± 0.15	34.0 ± 0.5
800 μM ADP	3.8 ± 0.3	38 ± 0.5	~43		
800 μM ADP, 20 mM P_i	1.3 ± 0.2	40 ± 0.5	~46		

[a] The results show how quenching varies with K^+ or NH_4^+ concentration when coupled with binding of ATP or ADP and the influence of 20 mM P_i. Most studies were conducted with 1.5 mM $MgCl_2$ which caused ~2% quenching (treated as 0% quenching and not included in Q_{max} or Q_{tot}). Q_{tot} includes quenching due to a fixed ADP or ATP level prior to any K^+. In the study with 1.0 mM ATP, the initial free Mg^{2+} concentration was 2.0 mM (caused 2.7% quenching) prior to the addition of ATP which increased quenching to ~14% prior to K^+ addition. Q_{max} does not include quenching by ATP or ADP in the absence of K^+, but Q_{tot} does include this quenching. Under all conditions, the values of the Hill coefficient, n, estimated in the fitting of data were between 1.0 and 1.2 with the exception of the experiment in which the K^+ concentration was varied with 800 μM ADP and 20 mM P_i, for which $n = 1.3 \pm 0.1$. [b] Error range based on the standard error from the Hill plots (eq 1) using Origin; asymmetric deviations are averaged. [c] Standard error. [d] Rounded to nearest 0.5%; error ranges of 0.5−3.0%.

<1.5 μM ATP·K^{3-} even at 100 mM K^+) and 200 μM ADP (170−160 μM ADP·Mg^- and 0−14.4 μM ADP·K^{2-} as the level of K^+ is varied from 0 to 80 mM). Na^+ ion did not replace K^+ ion in supporting quenching in the presence (Figure 2) or absence of P_i anion (data not shown). Therefore, specific ion effects rather than ionic strength effects are involved. Without P_i, quenching occurred with a near-hyperbolic dependence on the K^+ concentration, with lower K^+ concentrations being more effective with 100 μM ATP than with 200 μM ADP (Figure 2; see $L_{0.5}$ values in Table 1).

These data demonstrate a critical role of K^+ for strong Trp fluorescence quenching by ATP and ADP and that lower levels of ATP·Mg^{-2} than ADP·Mg^- promote tight binding of K^+. K^+-based stabilization of the ATP bound to PDHK2 is probably the primary basis for ATP being retained bound to PDHK2 upon dilution at 0 °C (cold-capture binding assay) and for the rate constant for ATP dissociation being smaller than k_{cat} (*11*). The $L_{0.5}$ for K^+ decreases with an increase in the level of ATP [e.g., 5, 50, 100, and 1000 μM (Table 1)].

P_i minimally altered K^+-dependent quenching of the Trp fluorescence of PDHK2 with ATP (slightly increased) but enhanced quenching with ADP (Figure 2 and Table 1). With 200 μM ADP, 20 mM P_i reduced the $L_{0.5}$ of PDHK2 for K^+ from 12 to 5.3 mM and with 800 μM ADP from 3.8 to 1.3 mM which equates with the $L_{0.5}$ for K^+ observed with 100 μM ATP. When 20 mM P_i was included, the quenching profiles generated with an increasing K^+ level were fit best by an n somewhat >1 (with 200 or 800 μM ADP, $n = 1.2$ or 1.3, respectively).

Effects of $MgCl_2$, ATP·Mg^{2-}, ADP·Mg^-, and Pyruvate in the Absence of K^+. In the studies described above, modest quenching by ATP and ADP was noted prior to addition of K^+. Additionally, there is very weak quenching by $MgCl_2$ (Supporting Information). When the ATP level was varied with different Mg^{2+} levels in the absence of K^+ ion (data with 10 mM $MgCl_2$ Supporting Information, Figure 2SA), the total quenching estimated for ATP was ~20% (~18% quenching beyond the initial quenching by 1.5 mM $MgCl_2$). With correction for the effects of $MgCl_2$, the analysis fit hyperbolic dependencies for ATP with a common K_d of 150 ± 20 μM for ATP (Table 2).

Table 2: Binding Parameters Estimated for Ligands by Fluorescence Quenching in the Absence of K^+ and P_i (except where P_i is indicated)

ligand varied at fixed ligand	K_d[a] (mM)	Q_{max}[a] (%)
ATP·Mg^{2-}	0.150 ± 0.02	20.0 ± 2
ADP·Mg^-	0.95 ± 0.25	17.5 ± 2.5
ADP·Mg^- and 20 mM P_i	2.15 ± 0.2	22.0 ± 1.5
pyruvate	0.460 ± 0.20	55.5 ± 0.7

[a] Values are rounded to the nearest 5 in the last decimal place.

In the analyses of quenching by ADP in the absence of K^+ using different fixed Mg^{2+} concentrations, the level of ADP·Mg^- was calculated for each ADP level (Supporting Information, Figure 2SB). With corrections for the effects of $MgCl_2$, we estimate a Q_{max} of 17.5 ± 2.5% and a K_d of 0.95 ± 0.25 mM for ADP·Mg^- in the absence of K^+ (Table 2). Addition of 20 mM P_i significantly increased the $L_{0.5}$ for ADP from 0.95 to ~2.2 mM while also supporting a modest increase in Q_{max} from ~17 to ~22% (Table 2). The increase in $L_{0.5}$ is in marked contrast to the effect of P_i in decreasing the $L_{0.5}$ with an elevated K^+ level (below).

Pyruvate was the only ligand that gave extensive quenching (Q_{max}) in the absence of K^+. The quenching profile with an increasing pyruvate level is well-behaved and hyperbolic (Figure 6A and Table 2). A K_d of ~460 μM was estimated for the binding of pyruvate to PDHK2 in the absence of other ligands.

Effects of K^+ Ion on ATP and ADP Binding to PDHK2 and Linkage Analysis. Inclusion of 100 mM K^+ caused ATP quenching of Trp fluorescence to have a 2.4-fold greater Q_{max} and an ~45-fold lower $L_{0.5}$ for ATP (Figure 3A and Table 3). Furthermore, the response at 100 mM K^+ exhibited positive cooperativity ($n = 1.7$). This contrasts with the near-hyperbolic response when the ATP level was varied in the absence of K^+ (Table 2) and for K^+-dependent quenching with fixed ATP levels (Table 1). Figure 4A shows a log−log plot of the change in $L_{0.5}$ for ATP with different fixed K^+ levels (from 0.1 to 400 mM) with data fit using eq 3. As

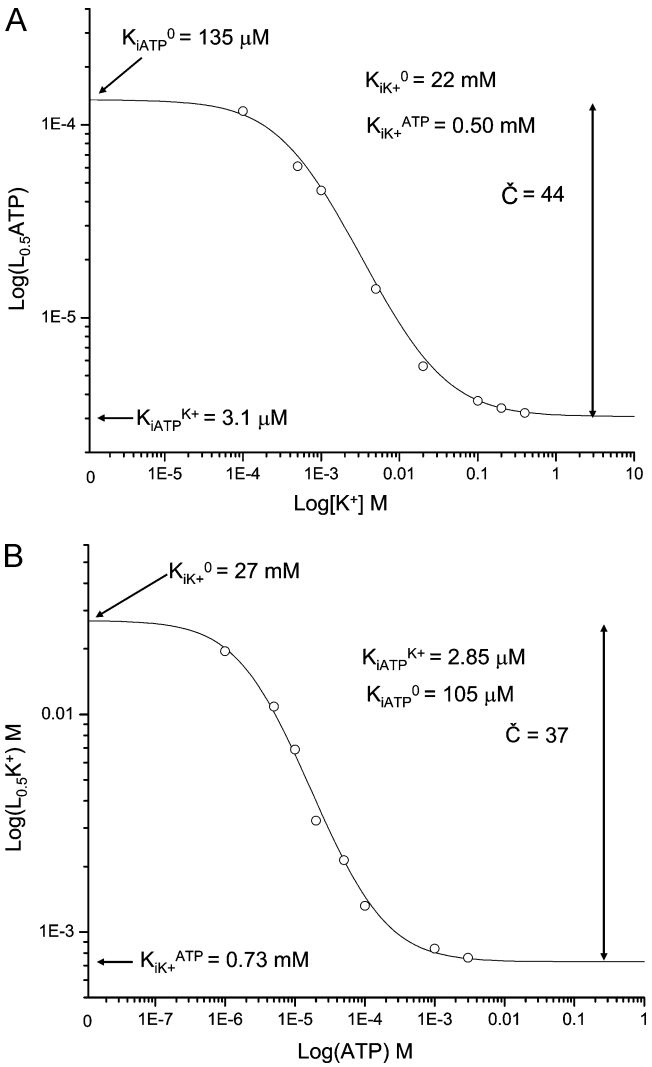

FIGURE 4: Dependence of the change in $L_{0.5}$ for K^+ on the concentration of ATP (A) and in $L_{0.5}$ for ATP on the concentration of K^+ (B). Data were analyzed with eq 3 as described in Experimental Procedures. The lowest level of 1 μM ATP (A) was the lowest order-of-magnitude concentration at which Trp fluorescence quenching could be measured without having a significant correction of the free concentration of ATP for bound ligand since at least 3 nM PDHK2 dimer was required for taking measurements with sufficient accuracy.

K^+ levels were decreased, the rise in $L_{0.5}$ for ATP (Figure 4A) occurred with a decrease in n (n = 1.7, 1.45, 1.15, and 0.98 at 100, 20, 5.0, and 1.0 mM K^+, respectively). The extrapolated y-intercept in Figure 4A gives a K_d for ATP in the absence of K^+ of 135 μM, and this fit to eq 3 yields a K_d of 3.1 μM ATP at saturating K^+ levels based the $\check{C}$ of ~44 which equals $K_{iATP}^0/K_{iATP}^{K^+}$ (fit 1, Table 4). The fit to eq 3 yielded a K_d of PDHK2 for K^+ in the absence of ATP of 22 mM. A binding affinity for K^+ of ~0.5 mM with a saturating level of ATP (Table 4) is derived on the basis of the value of $\check{C}$.

To further evaluate coupling and K_d values, the K^+ level was varied at fixed ATP levels from 1 to 3000 μM ATP and the resulting changes in $L_{0.5}$ for K^+ with fixed ATP levels analyzed in Figure 4B. The level of Mg^{2+} was varied to maintain essentially all ATP bound to Mg^{2+}. From fitting the data with eq 3 (fit 2, Table 4) and calculating all constants, we obtained a $\check{C}$ of 37 and K_d values for ATP of 105 and 2.85 μM for the transition from ATP binding to free PDHK2 and PDHK2·K^+, respectively. This was linked to a change from 27 to 0.73 mM for K^+ binding without and with ATP bound (fit 2, Table 4). In combination, the fitting of the data in panels A and B of Figure 4 supports an ~40-fold increase in affinity due to coupled binding of these ligands.

The fitting approach described above did not account for the weaker quenching in the binding of ATP alone. Data were globally fit using the random equilibrium assumption (eq 2) and the fitting conditions described in the footnotes of Table 4. The analysis set quenching of 18% for ATP binding to free PDHK2 (0% quenching with 1.5 mM Mg^{2+}) and 49% for formation of the ternary complex. Global fitting of the data when the ATP level was varied at different K^+ levels was performed with $K_{iK^+}^0 = K_{iB}^0$ (fit 3) or $K_{iATP}^0 = K_{iA}^0$ (fit 4) being varied until K_{iB}^a and K_{iA}^b values gave the smallest deviations along with obtaining the highest global correlation coefficient. Fitting of all the data when either the ATP or K^+ level was varied at fixed levels of the other ligand gave substantially lower values for ATP binding to free PDHK2 and higher values for K^+ binding but a poor global fit (footnote b of Table 4). This approach imposes a hyperbolic fit on the data analysis which agrees with profiles when the K^+ level was varied at different ATP levels but not the cooperative profiles for ATP at high K^+ levels. A rigorous fit to the cooperative ligand binding cannot be made for the PDHK2 dimer since we cannot assign the differences in quenching for different forms (e.g., EA vs EA/A, EA/B or EAB vs EAB/A, EAB/B, or EAB/AB). Regardless of the approach used to fit the data, substantial coupling in the binding of ATP and K^+ is supported by these linkage analyses. Overall on the basis of data in Tables 2 and 4, ATP is estimated to bind in the absence of K^+ with an affinity between 100 and 150 μM (average estimate of ~120 μM) and with an affinity of ~3 μM to PDHK2·K^+, yielding a $\check{C}$ of ~40.

In the presence of 100 mM K^+, the $L_{0.5}$ for ADP·Mg^- was ~57 μM with a Q_{max} of ~43%; the profile was hyperbolic ($n = 1.0 \pm 0.05$) (Figure 3A and Table 3). These data and those in which the K^+ level was varied at fixed ADP levels (Table 1) were globally fit using eq 2. Fit 5 in Table 4 set the K_d of 0.95 mM estimated for binding of ADP·Mg^- alone (Table 2) along with a Q_{max} of 15% for ADP binding in the absence of K^+. Although the values estimated for K_d and Q_{max} for ADP·Mg binding in the absence of K^+ have substantial error ranges, smaller errors are introduced in the global fit since formation of the PDHK2·ADP·Mg^-·K^+ complex dominates the quenching profile. The fit 6 analysis, which had a global correlation coefficient of 0.996, gave a $\check{C}$ of ~24 with a saturating K^+ level lowering the K_d for ADP to ~38 μM (Table 4). When K_{iB}^0 was varied to obtain the optimum fit, similar values were estimated (fit 6, Table 4). The independent estimate of K_d of ~40 mM for K^+ binding to PDHK2 (Table 4) should be more accurate than the value derived from ATP/K^+ studies because of the uniform near-hyperbolic nature of all the profiles along with accounting for different Q_{max} values by ADP bound with and without K^+. On the basis of the $\check{C}$ values of ~40 for ATP/K^+ and ~25 for ADP/K^+ (Table 4), substantially stronger coupling in the binding of ATP than ADP with K^+ is supported.

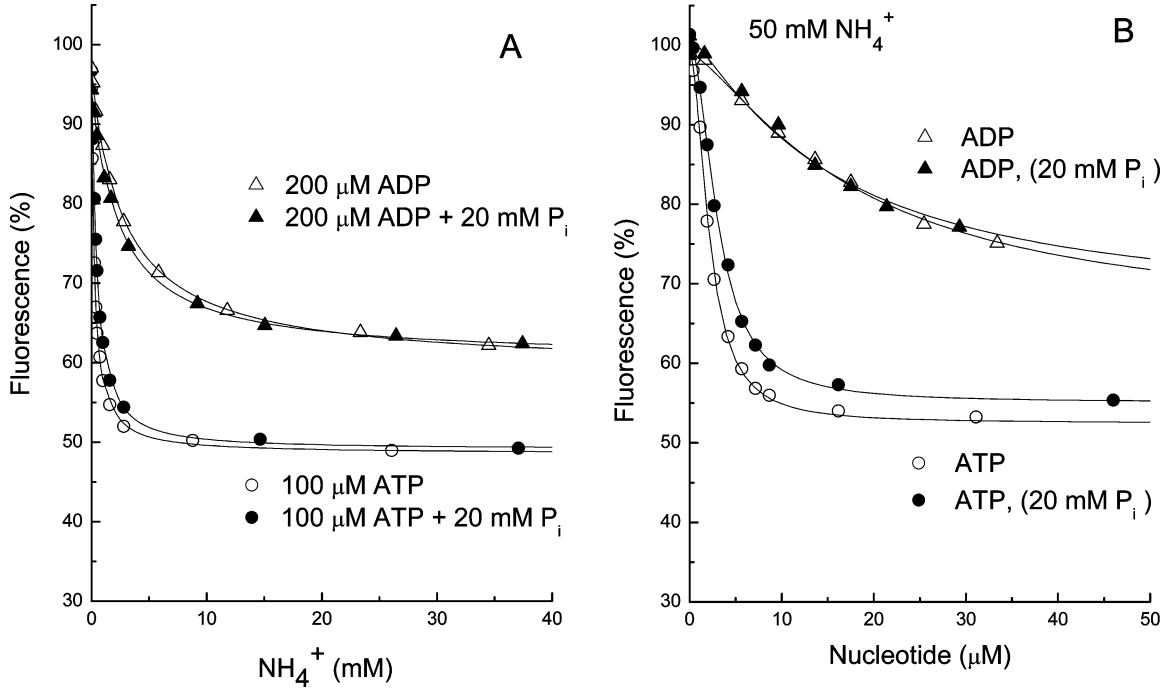

FIGURE 5: NH_4^+ ion-facilitated quenching by ATP and ADP with minimal effects of P_i. Panel A shows the dependence on NH_4^+ concentration and panel B the dependence on ATP and ADP at 50 mM NH_4^+. Measurements were taken under standard conditions, including 1.5 mM free Mg^{2+} prior, to addition of ATP or ADP as described in Experimental Procedures.

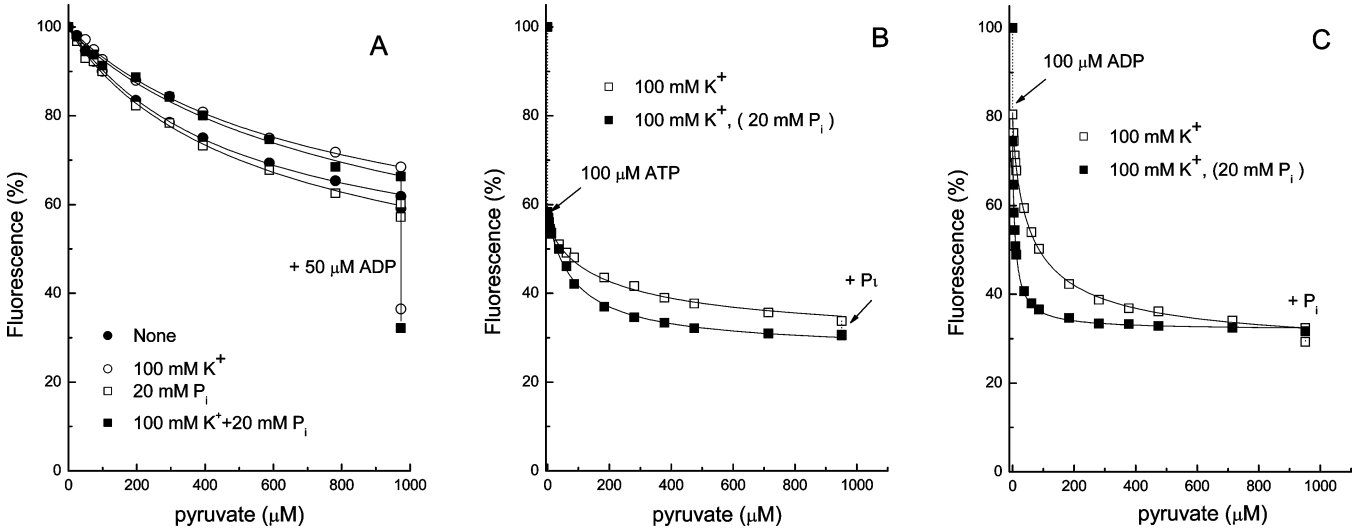

FIGURE 6: Pyruvate quenching of Trp fluorescence in the absence and presence of the indicated ions (A) and in the presence of 100 mM K^+ with 100 μM ATP (B) or 100 μM ADP (C) with or without 20 mM P_i. The studies in panel B and C were conducted with 1.5 mM Mg^{2+}; the level of ADP·Mg^- was ~70 μM in the study in panel C. Panel A also shows the effect of addition of 50 μM at the end of each titration. Panels B and C show the effects of addition of P_i to the titration lacking P_i; in panel B, the resulting point falls directly under the point for the other titration. Parameters are listed in Table 5.

Effect of P_i on Quenching. With 100 mM K^+, the $L_{0.5}$ for ADP·Mg^- was decreased by 20 mM P_i from 57 to 28 μM with little change in the maximal quenching by saturating ADP levels (Figure 3 and Table 3). In contrast, 20 mM P_i modestly increased the $L_{0.5}$ for ATP (Table 3). Further increasing the P_i level only slightly decreased the $L_{0.5}$ for ADP which remained 2-fold higher than that observed in potassium phosphate buffer (*13*). At pH 7.5, ~200 mM Hepes is required to provide the counterion for 100 mM K^+; possibly, this elevated Hepes level fosters an increase in $L_{0.5}$ for ADP. Results below (pyruvate effects) indicate that P_i is not binding where the γ-P_i of ATP binds at the active site.

Variation of the P_i level with 100 mM K^+ and 100 μM ADP invariably gave a complex profile in which fluorescence quenching at first increased and then decreased at higher P_i levels (Figure 3SA, Supporting Information). Fitting of the data with opposing hyperbolic changes gave an $L_{0.5}$ of ~3.2 mM P_i and a Q_{max} of 21% for the first phase (Table 3), and a very weak affinity (150 mM P_i) but with a substantial maximum fluorescence increase (~32%) in the second phase (see the Supporting Information). The decrease in fluorescence, in part, results from ADP binding since with an increasing P_i level there was some decrease in $L_{0.5}$ for ADP. The increase in fluorescence as the P_i level was increased

Table 3: Concentration Dependence for Quenching of Trp Fluorescence of PDHK2 by ATP, ADP, or P_i in the Presence of 100 mM K^+ or 50 mM NH_4^+

		with 100 mM K^+				with 50 mM NH_4^+			
fixed ligand(s)	varied ligand	$L_{0.5}$[a] (μM)	n[b]	Q_{max}[b] (%)	Q_{tot} (%)	$L_{0.5}$[a] (μM)	n[b]	Q_{max}[b] (%)	Q_{tot} (%)
	ATP	3.1 ± 0.07	1.7 ± 0.11	47.5 ± 1.0		1.7 ± 0.07	1.9 ± 0.15	46.2 ± 0.6	
20 mM P_i	ATP	3.9 ± 0.15	1.6 ± 0.11	49.5 ± 1.0		2.5 ± 0.07	1.9 ± 0.1	46 ± 0.5	
100 μM pyr	ATP	2.8 ± 0.08	2.05 ± 0.1	45.5 ± 0.9	~52	2.45 ± 0.05	1.72 ± 0.05	42.2 ± 0.3	54.5
100 μM pyr, 20 mM P_i	ATP	3.6 ± 0.1	1.95 ± 0.07	56.0 ± 1.0	~65	2.4 ± 0.1	2.0 ± 0.15	48.0 ± 0.8	~54
	ADP	72 ± 2.5	1.0 ± 0.05	43.0 ± 0.9		17.5 ± 1.0	1.35 ± 0.1	34.0 ± 0.8	
	as ADP·Mg^-	57.5							
20 mM P_i	ADP	35 ± 2	1.1 ± 0.05	44.5 ± 0.9		14.0 ± 0.6	1.4 ± 0.1	33 ± 0.6	
	as ADP·Mg^-	28							
100 μM pyr	ADP	18.0 ± 0.5	1.4 ± 0.05	51.0 ± 1.0	~58	11.3 ± 0.5	1.1 ± 0.06	40.5 ± 0.3	~53
	as ADP·Mg^-	14.5							
100 μM pyr, 20 mM P_i	ADP	4.0 ± 0.15	2.05 ± 0.1	62.0 ± 1.1	~67	4.45 ± 0.1	1.85 ± 0.06	52.5 ± 0.4	~60
	as ADP·Mg^-	3.2							
300 μM pyr, 20 mM P_i	ADP	2.6 ± 0.9	2.0 ± 0.2	18.3 ± 0.8	~70				
	as ADP·Mg^-	2.1							
100 μM ATP	P_i			<3	~45			<1[c]	~43
100 μM ATP and pyr	P_i	12.5 ± 0.7 mM	2.0 ± 0.2	15.0 ± 0.4	~64			<5[c]	~49
100 μM ADP	P_i	3.2 ± 0.3 mM[d]	1.0[d]	21.0 ± 2[d]	~40[d]	<8 mM, >2 mM[d]		~8[d]	~34[d]
100 μM ADP and pyr	P_i	0.85 ± 0.05 mM	1.3 ± 0.1	21.0 ± 0.4	~66	~1.5 mM		~12	~54

[a] Range based on the standard error from the Hill plot (eq 1) using Origin; asymmetric deviations are averaged. [b] Standard error. [c] With 50 mM NH_4^+ and inclusion of 100 μM ATP, there was no detectable effect of P_i in the absence of 100 μM pyruvate and the change due to P_i concentration with 100 μM pyruvate was too small to accurately measure the $L_{0.5}$. [d] Complex profiles, when the P_i concentration was varied with 100 μM ADP and either 100 mM K^+ or 50 mM NH_4^+, involved an initial decrease with and then an increase in fluorescence with a higher P_i concentration. The estimates of $L_{0.5}$ and Q_{max} for P_i with K^+/ADP that were derived from the first phase of quenching (Figure 3SA, Supporting Information) were estimated by a fit assuming a hyperbolic response is being opposed by a second hyperbolic response at a higher P_i concentration. With 50 mM NH_4^+, the sharp transition to a rise in fluorescence after a steep decrease occurred before there was sufficient data to fit the first phase of the profile. Minimum and maximum $L_{0.5}$ values were estimated. The Q_{max} with 50 mM NH_4^+ and the Q_{tot} with both monovalent cations reflect the maximum quenching observed as the P_i concentration was increased.

was not due to weakened ADP binding at higher P_i levels; indeed, tighter ADP binding was observed with 50 mM P_i with no decrease in Q_{max} (*13*). A potential cause of the biphasic response for P_i with ADP is considered in the Discussion. The second phase involving the fluorescence increase becomes more prominent when Nov3r is bound (companion paper[2]). In contrast, with 100 mM K^+ and 100 μM ATP, P_i had no effect on quenching (Figure 3SB, Supporting Information).

With the P_i level varied in the presence of both ADP and pyruvate, apparent tight P_i binding was observed ($L_{0.5} = 0.85$ mM); an increase in fluorescence was not observed at higher P_i levels. The best data fits required the introduction of positive cooperativity (Figure 3SA and Table 3). With ADP and pyruvate included at 100 μM, both increased ADP and pyruvate binding are predicted (~11 and ~27%, respectively, with 20 mM P_i using a rough estimate that treats the $L_{0.5}$ values in Table 3 as apparent dissociation constants). The binding of these ligands provides most of the observed increase in quenching with an increasing P_i level. Positive cooperativity may be the result of quenching produced by the binding of multiple ligands under these conditions (*35*). With saturating ADP and pyruvate levels (see the Supporting Information), P_i caused only ~3.2% additional quenching. Under these conditions (K^+, ADP, and pyruvate), P_i binding alters other interactions of PDHK2.[2]

With 100 μM ATP and 100 μM pyruvate, P_i-dependent quenching was observed with a higher $L_{0.5}$ of ~12.5 mM P_i (Figure 3SB and Table 3). Again, this P_i-dependent quenching increased in a highly cooperative manner ($n = 2.0$) with a minimal change in fluorescence above 40 mM P_i. No change in ATP binding is projected, but some increase in the level of pyruvate binding contributes to the P_i-dependent quenching and may contribute to the cooperative profile. Thus, the data suggest that P_i accumulated in the PDHK2·K^+·ADP·pyruvate·P_i complex with an ~10-fold tighter apparent binding affinity than in the PDHK2·K^+·ATP·pyruvate·P_i complex. However, an improved understanding of coupling and contributions of binding of other ligands to the observed profiles is needed to evaluate true differences in binding affinity.

NH_4^+ Ion Substitution for K^+. Unlike Na^+, NH_4^+ ion was effective in supporting quenching by 100 μM ATP and 200 μM ADP and did so with ~5-fold lower concentration dependencies than K^+ (Table 1 and Figure 5A). As with K^+, the $L_{0.5}$ for NH_4^+ was ~10 fold lower with 100 μM ATP (0.26 mM) than with 200 μM ADP (2.8 mM). In the presence of 200 μM ADP, P_i did not significantly decrease the $L_{0.5}$ for NH_4^+ (Figure 5A) as it did with K^+. Therefore, with 20 mM P_i and 200 μM ADP, the difference in $L_{0.5}$ for NH_4^+ and K^+ was reduced to ~2-fold, and there was a significantly higher Q_{max} with K^+ (Table 1).

With 50 mM NH_4^+ ion (Figure 5B), the $L_{0.5}$ values of PDHK2 for ATP and ADP were ~2- and ~4-fold lower than those obtained with 100 mM K^+ (Table 3). In the presence of 50 mM NH_4^+, there was little effect of K^+ on ATP and

Table 4: Binding Constants Estimated by Global Fitting of Multiple Data Sets Using Fractional Quenching by Single Ligands[a]

ligands varied (fit)								
A	B	K_{iA}^0 (μM)	K_{iB}[b] (mM)	K_{iB}^0 (mM)	K_{iA}[c] (μM)	$\check{C}$	Q_{tot} (%)	*c* and *d* ratios[c]
ATP·Mg^{2-}	K^+							
Figure 4A, fit 1[b]		135 ± 7	0.50	22 ± 2	3.1	44 ± 2		
Figure 4B, fit 2[b]		105 ± 10	0.73	27 ± 1	2.85	37 ± 1.5		
global fit 3[c]		101	0.78 ± 0.11	**28.0***	2.85 ± 0.1	36	49	c = 18/49, A varied
global fit 4[c]		**100***	0.72 ± 0.04	23	3.1 ± 0.3	32.5	49	c = 18/49, B varied
ADP·Mg^-	K^+							
global fit 5[d]		**950**	1.68 ± 0.11	42	38 ± 3	25	43	c = 15/43, d = 0
global fit 6[d]		935	1.65 ± 0.25	**40***	38.5 ± 1.1	24	43	c = 15/43, d = 0
pyruvate	ADP·Mg^-							
global fit 7[e]		**460**	0.450 ± 0.055	0.830	295 ± 45	1.55	69	c = 55.5/69, d = 15/69
global fit 8[e]		585	0.400 ± 0.070	**0.940***	250 ± 40	2.35	69	c = 55.5/69, d = 15/69

[a] When values were set in the fitting of data, they are shown in bold; if the set value was varied to minimize the error, it is shown with an asterisk. When values are calculated from values obtained in fitting using the relationships $K_{iA}^0 K_{iB}^a = K_{iB}^0 K_{iA}^b$ or $\check{C} = K_{iA}^0/K_{iA}^b = K_{iB}^0/K_{iB}^a$, the answers are shown without experimental errors included. [b] Data were fit using eq 3. In using eq 3, A is K^+ and B is ATP for fit 1 (Figure 4A) and A is ATP and B is K^+ for fit 2 (Figure 4B). K_{iB}^a and K_{iA}^b values were calculated from the fit values. [c] Data were fit using the random equilibrium (eq 2) or modified forms of eq 2 (i.e., if K_{iB}^0 was known while keeping this equilibrium constant). Whether A or B is varied, *c* and *d* are the fraction of Q_{max} for EAB by forming EA and EB, respectively, based on values experimentally determined but not including the quenching by 1.5 mM Mg^{2+}. In fits 3 and 4, the full set of data in which the ATP level was varied at different levels of K^+ was fit. The fitting approach shown varied the value of $K_{iB}^0 = K_{iK^+}^0$ (fit 3) or $K_{iA}^0 = K_{iATP}^0$ (fit 4) to minimize errors in fitting K_{iB}^a and K_{iA}^b values (see Experimental Procedures). K_{iB}^0 (fit 3) or K_{ia}^0 (fit 4) and $\check{C}$ were calculated from these results. The data in which either the ATP level was varied at a fixed K^+ level or the K^+ level was varied at a fixed ATP level were also globally fit using the same fitting approach as in fit 3. That fit gave a significantly poorer global correlation coefficient of 0.97 vs >0.985 for fits 3 and 4 and yielded a lower K_{iATP}^0 (67 μM) and a higher $K_{iK^+}^0$ (40 mM). [d] All the data with ADP (ADP·Mg^- calculated) or K^+ levels varied at fixed levels of the other ligand were fit with eq 2. In fit 5, a global correlation coefficient of 0.999 was obtained using the K_{iADP}^0 value of 950 μM (Table 2). In fit 6, $K_{iK^+}^0$ was varied to minimize errors ($K_{iK^+}^{ATP}$ and $K_{iATP}^{K^+}$ with smallest deviations along with the best global correlation coefficient). [e] All data when the ADP or pyruvate level was varied at fixed levels of the other ligand were fit using eq 2. In fit 7, the estimated K_d of 460 μM for pyruvate was used; in fit 8, the level of ADP was varied until the smallest error in the global fit and K_{ipyr}^0 were obtained.

ADP binding affinity, supporting these monovalent cations acting at the same site (data not shown). In contrast to the results with 100 mM K^+, inclusion of 20 mM P_i had a minimal impact when the ADP level was varied with 50 mM NH_4^+ (e.g., Figure 5B and Table 3). Total quenching by ADP was not as high with 50 mM NH_4^+ as with 100 mM K^+ whether ADP was added alone or with 20 mM P_i, or with 100 μM pyruvate and 20 mM P_i. However, similar Q_{max} values were achieved with higher pyruvate levels. Therefore, NH_4^+ ion was effective at lower concentrations than K^+ in supporting ATP/ADP quenching of the Trp fluorescence of PDHK2, but NH_4^+ did not match the capacity of K^+ to foster P_i-enhanced quenching by ADP.

Highly Modulated Fluorescence Quenching by Pyruvate. As described above, pyruvate in the absence of any K^+ or NH_4^+ (Figure 6A) gave significant quenching of Trp fluorescence (Table 2). Addition of 20 mM P_i modestly increased Q_{max} but also slightly increased the $L_{0.5}$ for pyruvate-dependent quenching (Figure 6A and Table 5). K^+ also caused a small increase in the $L_{0.5}$ of PDHK2 for pyruvate without a significant increase in Q_{max} (Figure 6A and Table 5). The $L_{0.5}$ for pyruvate was further increased by the combination of 100 mM K^+ and 20 mM P_i (Figure 6A and Table 5). In contrast, inclusion of 50 mM NH_4^+, alone, did not increase the $L_{0.5}$ for pyruvate; including 20 mM P_i with NH_4^+ caused a definite but modest increase in $L_{0.5}$ and Q_{max} (Table 5).

Without K^+ ion, 1.0 mM ADP (0.73 mM ADP·Mg^-) had a minimal effect on pyruvate quenching. The binding dissociation constants shown in the bottom data set of Table 4 were obtained from fitting of these data with random equilibrium binding of pyruvate and ADP·Mg^- and using as Q_{max} values: 15% quenching by ADP·Mg^- alone, 55.5% by pyruvate alone, and 69% by the combination. Using the K_d of 460 μM for binding of pyruvate, alone, to PDHK2 (Table 2), a K_d for binding of ADP·Mg^- to free PDHK2 of 830 μM was estimated (fit 7, Table 4). This indicates that there is little or no coupling in binding of ADP and pyruvate in the absence of K^+ and P_i. In close agreement with Table 2, a K_d of 940 μM for ADP·Mg^- gave the lowest error ranges (fit 8), and this fit yielded a value of 585 μM for K_d for binding of pyruvate to PDHK2, somewhat above the measured value. Fit 8 supported slightly greater but still very weak coupling ($\check{C}$ < 2.4) in the binding of ADP and pyruvate in the absence of K^+ and P_i (Table 4).

In the absence of K^+, the combination of 20 mM P_i and 1.0 mM ADP gave only a 4-fold decrease in $L_{0.5}$ for pyruvate (Table 5). In marked contrast, in potassium phosphate buffer, ADP caused 150-fold decreases in $L_{0.5}$ for pyruvate (*13*). ATP caused only a 10-fold effect using potassium phosphate (*13*). Those results had raised questions of whether P_i acts only with ADP and not with ATP and how the role of K^+ in pyruvate binding is changed by other ligands.

With 100 mM K^+, other ligands caused marked changes in the $L_{0.5}$ values for pyruvate. Just as K^+ alone or P_i alone increased the $L_{0.5}$ for pyruvate (Table 5), the combination caused a further increase. With K^+, 100 μM ATP supported an only ~3-fold decrease in the $L_{0.5}$ for pyruvate (Figure 6B) but with an increase in Q_{tot} and introduction of some negative cooperativity (n = 0.82). However, ATP with P_i, via a K^+-dependent allosteric mechanism, lowered the $L_{0.5}$ for pyruvate by ≥10-fold below that found with P_i/K^+ (Figure 6B and Table 5). This strongly indicates that P_i produces this effect by binding at a location separate from the binding site of the γ-phosphate of ATP at the active site.

Table 5: Quenching of Trp Fluorescence by Pyruvate and Effects of Various Additions on Pyruvate Quenching[a]

		pyruvate varied		
fixed ligand(s)	cation level[b]	$L_{0.5}$[a] (μM)	Q_{max} (%)	Q_{tot} (%)
none	none	460 ± 20	55.3 ± 0.5[d]	
20 mM P_i		565 ± 30	64 ± 3[d]	
1 mM ADP		420 ± 10	65 ± 2.5[d]	~72
1 mM ADP, 20 mM P_i		117 ± 4	61.0 ± 1.2[d]	~68
none	100 mM K^+	770 ± 30	57 ± 2[d]	
20 mM P*i*		1070 ± 210	69 ± 6[d]	
100 μM ATP		210 ± 15	30.0 ± 1.2[c]	~67
100 μM ATP, 20 mM P_i		84 ± 8	30.0 ± 0.6[c]	~71
100 μM ADP		55 ± 2.5	51.0 ± 1.0[c]	~70
200 μM ADP		18.3 ± 1	33.0 ± 1.5[c]	~68
100 μM ADP, 20 mM P_i		8.5 ± 0.2	43.0 ± 0.9[c]	~76
200 μM ADP, 20 mM P_i		8.3 ± 0.25	29.0 ± 0.9[c]	~74
none	50 mM NH_4^+	395 ± 20	58 ± 2[d]	
20 mM P_i		530 ± 10	64.0 ± 1.0[d]	
100 μM ATP		160 ± 10	22 ± 2[c]	~68
100 μM ATP, 20 mM P_i		155 ± 8	27 ± 3[c]	~72
100 μM ADP		115 ± 15	38 ± 1.5[c]	~68
100 μM ADP, 20 mM P_i		32 ± 1.5	39 ± 1.5[c]	~70

[a] Values were derived with eq 1 using Origin. In the cases where the $L_{0.5}$ exceeds 300 μM, Q_{max} values estimated from reciprocal plots ($1/Q$ vs [pyruvate]$^{-1}$) and standard deviations are shown. All estimates of n were within the range of 1.0 ± 0.2; n values of ≤0.85 were estimated when the pyruvate concentration was varied with 100 mM K^+ and 100 μM ATP or 200 μM ADP. [b] Other than Tris cation. [c] Standard error. [d] Standard deviation for Q_{max} from the reciprocal plot.

These results are in accord with K^+, ATP, and pyruvate enhancing P_i binding above. Due to the qualitatively similar effects with K^+ and pyruvate, P_i is assumed to bind at a common site in producing linked effects with ADP and ATP. However, with 100 μM pyruvate with or without P_i, the $L_{0.5}$ values estimated for ATP were not reduced below the $L_{0.5}$ for ATP with just 100 mM K^+; the responses with 100 μM pyruvate were highly cooperative [$n \sim 2.0$ (Table 3)]. Again, cooperativity may result from enhanced pyruvate binding and quenching as ATP levels are increased. Using higher but nonsaturating pyruvate levels and 20 mM P_i, $L_{0.5}$ values for ATP were not decreased below the value of 3.6 μM found with 100 μM pyruvate, but ATP-dependent quenching could be observed only over small intervals.

In studies that included P_i, ADP had a pronounced effect on pyruvate binding or inhibition of PDHK2 (*11*, *13*). With 100 mM K^+, even in the absence of added P_i, 100 μM ADP supported a ≥10-fold decrease in $L_{0.5}$ for pyruvate to ~55 μM (Figure 6C and Table 5), exceeding the effect of ATP and P_i in lowering the $L_{0.5}$ for pyruvate. With 20 mM P_i also included (Figure 6C), the $L_{0.5}$ for pyruvate was further decreased to 8.5 μM in the presence of 100 μM ADP (Table 5). Increasing the ADP concentration to 200 μM did not further decrease the $L_{0.5}$ for pyruvate. Therefore, coupled binding with ADP, K^+, and P_i results in a pronounced gain in pyruvate binding. In agreement with linked effects with these ligands, the $L_{0.5}$ for ADP·Mg^- (Figure 3 and Table 3) was reduced 2-fold by inclusion of 100 μM pyruvate and further reduced ~9 fold by additionally including 20 mM P_i (Figure 3B and Table 3). With 300 μM pyruvate (near saturating under these conditions), the $L_{0.5}$ for ADP was reduced to 2.6 μM (2.1 μM ADP·Mg^{2+}) with 20 mM P_i and 100 mM K^+. Clearly, there is coupled binding of these ligands, but the linkages are not simple (see the Discussion).

Although 50 mM NH_4^+ was very effective in supporting ATP and ADP binding and pyruvate-enhanced ADP binding (Table 3), the $L_{0.5}$ values for pyruvate with 100 μM ADP or 100 μM ADP and 20 mM P_i were significantly higher than those observed with these ligands in the presence of 100 mM K^+ (Table 5). With 50 mM NH_4^+, P_i had small effects on pyruvate, ATP, or ADP binding alone. However, along with ADP, P_i significantly lowered the $L_{0.5}$ for pyruvate with NH_4^+ replacing K^+. Thus, with NH_4^+, P_i has significant effects on the coupled binding of ADP and pyruvate (Tables 3 and 5); inclusion of ADP has a particularly large effect in decreasing the $L_{0.5}$ for pyruvate with P_i (16.5-fold) compared to a value of 3.4-fold in the absence of P_i (Table 5).

Changes in the Kinetic Properties of PDHK2 with Added Ions. We previously found that a change from a buffer with a low K^+ level (~12 mM) to one with an elevated K^+ concentration (~103 mM), ~13 mM P_i invariant, decreased the K_m for ATP and the K_i for ADP of PDHK2 by ~3-fold along with a decrease in k_{cat} that was nearly as large (*11*). In the complete absence of K^+ and P_i, the K_m for ATP was elevated to 240 μM (Figure 4S, Supporting Information, and Table 6) which is somewhat above the K_d value estimated for ATP. Under these conditions, PDHK2 is catalytically very active with a V_{max} of 815 nmol min^{-1} mg^{-1} ($k_{cat} = 1.25$ s^{-1}) (Table 6). Therefore, functional use of ATP does not depend on K^+ ion. Addition of 100 mM K^+ or 50 mM NH_4^+ modestly reduced the K_m for ATP to ~140 or ~90 μM, respectively (Table 6). With 100 mM K^+, the K_m that is appreciably higher (Table 6) than the K_d for ATP (Tables 3 and 4) is expected on the basis of the proposed ordered reaction mechanism (*11*),[3] but kinetic parameters may also be influenced by the additional interactions of PDHK2 with E2 and E1 (see the Discussion and the companion paper[2]).

Within experimental error, 20 mM P_i had no effect in the absence of K^+ on the K_m for ATP. With 100 mM K^+, 20 mM P_i supported a 3-fold decrease in the K_m for ATP with a similar decrease in V_{max}. Kinetic studies found that this was due to P_i functioning as an uncompetitive inhibitor ($^{app}K_i \sim 12$ mM). This suggests that K^+-dependent P_i binding is preferential with either PDHK2·ATP, PDHK2·ADP, or both. The binding studies described above support P_i binding

Table 6: Changes in Kinetic Parameters of PDHK2 with Inclusion of Various Ions and Changes in Pyruvate Inhibition[a]

ion	K_m(ATP) (μM)	K_m(ATP)/$L_{0.5}$(ATP)	V_{max} (nmol min^{-1} mg^{-1})	k_{cat}/K_m (s^{-1} M^{-1})	% inhibition by pyruvate[d] 100 μM	300 μM
none[b]	240 ± 20	~1.6[c]	815 ± 55	0.52×10^4	10 ± 4	23 ± 5
K^+ (100 mM)[b]	143 ± 8	46	1125 ± 30	1.2×10^4	21 ± 3	44 ± 4
NH_4^+ (50 mM)	90 ± 7	53	640 ± 20	1.1×0^4		
P_i (20 mM)	265 ± 30	ND	920 ± 80	0.53×10^4	13 ± 4	34 ± 2
K^+ (100 mM), P_i (20 mM)	53 ± 9	14	430 ± 25	1.24×10^4	74 ± 1	89 ± 1.5

[a] All kinetic constants are apparent constants; however, increasing the concentration of E2-bound E1 did not significantly increase initial rates. [b] Data in Figure 4S of the Supporting Information). [c] Based on the K_d estimated by fluorescence quenching in the absence of K^+ (Table 2). Averaging the estimates of the K_d for ATP binding to free PDHK2 in coupling studies (Table 4) with this value gives 118 ± 23 μM, giving a K_m(ATP)/$L_{0.5}$(ATP) ratio of ~2. [d] Data including variation in control activities in Figure 5S of the Supporting Information.

primarily to PDHK2·ADP in the absence of pyruvate. In agreement with ADP dissociation being rate-limiting in PDHK2 catalysis with elevated K^+ levels and 13 mM P_i (*11*) and with the larger decrease in $L_{0.5}$ for pyruvate with ADP than with ATP in the presence of K^+/P_i (Table 5), the degree of pyruvate inhibition was markedly increased when 20 mM P_i was included along with 100 mM K^+ (Table 6). Without K^+, there was very weak pyruvate inhibition that was minimally enhanced by 20 mM P_i (Figure 5S); however, with 100 mM K^+, P_i greatly enhanced pyruvate inhibition (Figure 5S). The results are consistent with P_i slowing catalytic turnover by favoring retention of pyruvate and ADP.

DISCUSSION

Subsequent to the finding that K^+ ion decreased the K_m for ATP and the K_i for ADP (*25*), several studies reported substantial effects of ions on PDHK catalysis and regulation (*11*, *12*, *26*, *27*, *36*). As indicated in the introductory section, crystal structures of the related BCDK and PDHK3·L2 structures with ATP or ADP bound had a K^+ ion held at the active site with the α-phosphate of the adenine nucleotide contributing to K^+ chelation (*24*, *28*). Using potassium phosphate buffer, ATP, ADP, or pyruvate strongly quenched the fluorescence of Trp383 of PDHK2 (*13*). Here we establish that the quenching by ATP and ADP requires the monovalent cations K^+ and that this can be replaced by lower levels of NH_4^+ ion but not Na^+. In contrast, pyruvate quenched PDHK2 Trp fluorescence without K^+ and pyruvate binding was not enhanced by K^+.

The coupled binding of K^+ with other ligands had not been treated quantitatively with any PDK isoform prior to this study. We have determined the binding dissociation constants for the highly coupled binding of ATP/ADP and K^+ by PDHK2. We have found that for ADP enhancing pyruvate binding requires K^+ for a significant (14-fold) effect. However, this is a much weaker coupling effect than that found in the prior studies conducted with potassium phosphate buffer (*13*). We have established that the deficit is due to substantial effects of P_i which amplify the effects of ADP to yield the 125-fold decrease in the $L_{0.5}$ for pyruvate. This K^+-dependent result gains from the transition from P_i weakening pyruvate binding to enhancing pyruvate binding in the presence of ADP. Using fluorescence quenching, we have provided the first estimates of the K_d for binding of ATP, ADP·Mg^-, K^+, and pyruvate to free PDHK2.

With elevated K^+ and P_i using E2-bound E1 as a substrate, PDHK2 catalyzes a nonequilibrium steady state reaction relatively insensitive to the concentration of the second substrate (E1) (*11*); binding of PDHK2 to the lipoyl domains of E2, particularly the L2 domain (*9*, *21*), is required for this outcome. In the absence of E2, PDHK2 catalysis is minimally sensitive to effectors, including pyruvate (*9*), and the reaction has a very high K_m for E1 (*11*). These properties prevent linkage analysis by steady state kinetic investigations. As a consequence, analysis of allosteric interactions by binding studies becomes particularly important. However, quantitative characterization of the allosteric coupling in the binding of different ligands by studies of fluorescence quenching is made challenging even for just two ligands due to K^+ or P_i, alone or in combination, not causing significant quenching of the Trp fluorescence. Additionally, ATP or ADP caused weaker quenching in the absence of K^+ (or NH_4^+) ion. One estimate of ~50 for coupling constant $\check{C}$ for ATP and K^+ binding is derived from our estimates of the K_d values for ATP binding in the absence of K^+ [150 μM (Table 2)] and with 100 mM K^+ [3.1 μM (Table 3)]. Lower values of $\check{C}$ of 37−44 were obtained from the data in Figure 4. The best estimate of ~40 mM for binding of K^+ to free PDHK2 was derived from global fitting of the uniformly hyperbolic data from studies of ADP/K^+ fluorescence quenching. We find somewhat stronger coupling of K^+ with ATP than with ADP (Table 4). A large impact of K^+ on the affinities of ATP and ADP at the active site of PDHK2 is predicted with K^+ levels of 100−130 mM which are found within the mitochondrial matrix space.

These coupling results provide mechanistic insights that help to explain kinetic studies in which with elevated K^+ levels (113 mM) the rate of ATP dissociation was determined to be slower than k_{cat} and ADP dissociation was found to be a rate-limiting step (*11*). Here we show that PDHK2 is highly active in the complete absence of K^+. However, effector-altered modulation of PDHK2 activity requires elevated K^+ levels. In agreement with a nonequilibrium mechanism in which ADP dissociation limits PDHK2 catalysis, we find that the K_m for ATP is 143 μM with 100 mM K^+, well above the K_d of ~3 μM for binding of ATP. A change toward a near-equilibrium mechanism in the absence of K^+ is indicated by the K_m for ATP of ~250 μM and the K_d for ATP of ~120 μM. We propose that the more rapid dissociation of ATP and even weaker binding of ADP in the absence of K^+ lead to the loss of regulatory sensitivity to inhibitory and stimulatory effectors of PDHK2 activity (*9*, *11*, *12*).

The $L_{0.5}$ of 460 μM for pyruvate binding alone should be a good measure of its equilibrium binding affinity. Although

our results demonstrate that pyruvate binds to free PDHK2 in the absence of K^+ or adenine nucleotides, the much tighter pyruvate binding along with K^+ and ATP or ADP are in accord with past evidence that pyruvate is as an uncompetitive inhibitor that binds to the PDHK2·ATP·Mg·K complex and even more tightly to the PDHK2·ADP·Mg·K complex (*11*). Therefore, potent pyruvate inhibition issues from K^+ enhancing the binding of ATP and ADP. In contrast in the absence of K^+, we find only slight coupling in the binding of ADP and pyruvate (Table 4).

In general, whether ADP, P_i, or pyruvate is the varied ligand, marked reductions in $L_{0.5}$ were observed when the full set of these ligands was included with 100 mM K^+, but the transitions and linkages are complicated. By inclusion of K^+, P_i, and 300 μM pyruvate, the $L_{0.5}$ for ADP was reduced ~530-fold from ~950 to 1.8 μM ADP·Mg^{2+}. There was a 10-fold smaller total decrease in the $L_{0.5}$ for pyruvate (from 460 to 8.5 μM). However, due to the negative effects of K^+/P_i on pyruvate binding, ADP fostered a 125-fold decrease in $L_{0.5}$ for pyruvate (from 1070 to 8.5 μM). The 13-fold decrease in the $L_{0.5}$ for ADP upon addition of 300 μM pyruvate is modest by comparison. A conditional linkage analysis (with 100 mM K and 20 mM P_i) reveals a >8-fold discrepancy ($K_{ipyr}{}^0K_{iADP}{}^{pyr} \gg K_{iADP}{}^0K_{ipyr}{}^{ADP}$); the second K_d in each term was obtained by extrapolation using eq 3, albeit with limited data (1.4 μM was the minimal K_d for ADP estimated at saturating pyruvate levels). It is clear that the linkage between ADP/K^+ and P_i greatly alters the effect of P_i on pyruvate binding. Improved understanding of P_i binding is needed to fully evaluate the coupling in the binding of these ligands.

With just ADP and K^+, we have repeatedly observed a complex Trp fluorescence profile with the P_i level varied in which low levels of P_i quenched fluorescence but higher P_i levels increased Trp fluorescence. Future studies will be needed to determine the cause of this effect. In the companion paper,[2] Nov3r favors the transition from quenching to enhancing fluorescence at lower P_i levels. It seems either that P_i binds at two sites in PDHK2 subunits or binding of P_i to one subunit along with ADP greatly alters binding of P_i to the second subunit of the PDHK2 dimer. With ADP, K^+, and pyruvate, only quenching was observed and a low $L_{0.5}$ of 0.85 mM P_i was obtained (Table 3). P_i binding greatly enhances ADP and pyruvate inhibition (Figure 5S) (*11*), and stimulation of PDHK2 activity involves reversing ADP, P_i, or Cl^- (or pyruvate) inhibition (*12*). The companion paper[2] uncovers critical roles of P_i that are also K^+-dependent and involve coupled binding of P_i with other ligands. P_i appears to play a special adapter role in intersite communication that can only be fully dissected by identifying P_i binding sites in PDHK2. Like ADP, an increased intramitochondrial P_i levels is a very important indicator of energy demand.

NH_4^+ often binds enzymes at K^+ binding sites; NH_4^+ ion has an ionic radius between those of K^+ and Rb^+, and the proton character of the NH_4^+ ion often leads to unique binding, including tighter or weaker binding at different K^+ sites (e.g., refs *37*−*39*). We find that lower levels of NH_4^+ supported tight ADP/ATP binding and effective quenching of Trp fluorescence. The interaction of NH_4^+ with PDHK2 was distinguished from that by K^+ in its inability to replicate the capacity of K^+ to support P_i-enhanced binding of ADP. Only when ADP and pyruvate were included did NH_4^+ ion show any linkage to P_i. An intracellular role of NH_4^+ in regulating PDHK2 activity seems unlikely.[4] A second K^+ site, important for PDHK2 binding to L2, is indicated in the companion paper[2] and is distinguished by NH_4^+ ion being quite ineffective at this site.

Modeling of K^+ binding to the crystal structures of PDHK2 indicated that the structure with ADP and DCA bound positions residues for greatly favored chelation of K^+ at the active site as compared to the positioning in the apoenzyme or enzyme with ATP and Nov3r bound when crystals were developed under the same (low K^+) conditions (*22*). Uncertainties arise in interpreting those data because crystallization captures specific conformations among a larger ensemble. Nevertheless, this interpretation is bolstered by our finding that the binding of ADP and pyruvate is stabilized by firm K^+ binding which almost certainly occurs at the active site. The combined allosteric coupling of K^+, ADP, pyruvate, and P_i explains the 150-fold decrease in $L_{0.5}$ for pyruvate due to inclusion of ADP in studies conducted in potassium phosphate buffer (*13*). Extensive studies will be needed to quantitatively evaluate the changes in binding affinities and specific intersite couplings at work in these higher-order complexes and the structural requirements that underpin acquisition of these intersite linkages.

Overall, we have found that K^+ enhances ATP and ADP binding and that the enhancement in pyruvate binding by ATP and especially ADP is K^+-dependent. We have shown that the effect of P_i in enhancing binding by ADP and the combination of ADP and pyruvate is also K^+-dependent. The ADP-dependent change from P_i weakening to strengthening pyruvate binding probably results from K^+-aided ADP binding altering P_i binding at the same site or fostering P_i acting at an additional site. These linked binding roles of K^+ and P_i result in trapping of ADP and pyruvate on PDHK2 and thereby produce the potent (synergistic-appearing) inhibition of PDHK2 activity by ADP and pyruvate. The companion paper[2] shows major effects of P_i on lipoyl domain binding by PDHK2, in promoting the conversion of PDHK2 dimer to a tetramer, and in the transmission of allosteric effects from the Nov3r/lipoyl binding site of PDHK2.

[4] When there is a need to neutralize acids excreted in the kidney, NH_4^+ ion and α-ketoglutarate are generated from glutamine. While the majority of the α-ketoglutarate produced is normally used in gluconeogenesis, some conversion of phosphoenolpyruvate to pyruvate followed by the PDC reaction helps meet the energy demands of the kidney. PDC catalysis (and activation) is required for full oxidative utilization of α-ketoglutarate by repeated full rounds of the citric acid cycle which consumes only acetyl-CoA. Elevation of NH_4^+ ion levels has been linked to activation of liver PDC (*40*). However, NH_4^+-enhanced ADP (and pyruvate) inhibition of PDHK2 which favors PDC activation would not appear to have physiological significance since the level of K^+ within the mitochondrial matrix space remains near saturating for supporting these regulatory effects.

ACKNOWLEDGMENT

We thank Dr. Aron W. Fenton (University of Kansas Medical Center, Kansas City, KS) for his advice and independent analysis of some of our data.

SUPPORTING INFORMATION AVAILABLE

Effects of ions (K^+, NH_4^+, Na^+, and $MgCl_2$) on Trp fluorescence quenching of PDHK2 (Figure 1S), fluorescence

quenching by ATP·Mg and ADP·Mg in the absence of monovalent cations (Figure 2S), effects of P_i level on quenching with ADP or ATP without and with pyruvate (Figure 3S), the change in kinetic parameters of E2-bound PDHK2 with the ATP level varied with or without K^+ (Figure 4S), and effects of ions on pyruvate inhibition of PDHK2 (Figure 5S). This material is available free of charge via the Internet at http://pubs.acs.org.

REFERENCES

1. Randle, P. J. (1986) Fuel selection in animals, *Biochem. Soc. Trans. 14*, 1799−1806.
2. Randle, P. J. (1995) Metabolic fuel selection: General integration at the whole-body level, *Proc. Nutr. Soc. 54*, 317−327.
3. Roche, T. E., Baker, J. C., Yan, X., Hiromasa, Y., Gong, X., Peng, T., Dong, J., Turkan, A., and Kasten, S. A (2001) Distinct regulatory properties of pyruvate dehydrogenase kinase and phosphatase isoforms, *Prog. Nucleic Acid Res. Mol. Biol. 70*, 33−75.
4. Roche, T. E., and Hiromasa, Y. (2007) Pyruvate dehydrogenase kinase regulatory mechanisms and inhibition in treating diabetes, heart ischemia, and cancer, *Cell. Mol. Life Sci. 64*, 830−849.
5. Gudi, R., Bowker-Kinley, M. M., Kedishvili, N. Y., Zhao, Y., and Popov, K. M. (1995) Diversity of the pyruvate dehydrogenase kinase gene family in humans, *J. Biol. Chem. 270*, 28989−28994.
6. Rowles, J., Scherer, S. W., Xi, T., Majer, M., Nickle, D. C., Rommens, J. M., Popov, K. M., Harris, R. A., Riebow, N. L., Xia, J., Tsui, L.-C., Bogardus, C., and Prochazka, M. (1996) Cloning and characterization of PDK4 on 7q21.3 encoding a fourth pyruvate dehydrogenase kinase isozyme in human, *J. Biol. Chem. 271*, 22376−22382.
7. Wu, P., Blair, P. V., Sato, J., Jaskiewicz, J., Popov, K. M., and Harris, R. A. (2000) Starvation increases the amount of pyruvate dehydrogenase kinase in several mammalian tissues, *Arch. Biochem. Biophys. 381*, 1−7.
8. Bowker-Kinley, M. M., Davis, W. I., Wu, P., Harris, R. A., and Popov, K. M. (1998) Evidence for existence of tissue-specific regulation of the mammalian pyruvate dehydrogenase complex, *Biochem. J. 329*, 191−196.
9. Baker, J. C., Yan, X., Peng, T., Kasten, S. A., and Roche, T. E. (2000) Marked differences between two isoforms of human pyruvate dehydrogenase kinase, *J. Biol. Chem. 275*, 15773−15781.
10. Korotchkina, L. G., and Patel, M. S. (2001) Site specificity of four pyruvate dehydrogenase kinase isozymes toward the three phosphorylation sites of human pyruvate dehydrogenase, *J. Biol. Chem. 279*, 37223−37229.
11. Bao, H., Kasten, S. A., Yan, X., and Roche, T. E. (2004) Pyruvate dehydrogenase kinase isoform 2 activity limited and further inhibited by slowing down the rate of dissociation of ADP, *Biochemistry 43*, 13432−13441.
12. Bao, H., Kasten, S. A., Yan, X., Hiromasa, Y., and Roche, T. E. (2004) Pyruvate dehydrogenase kinase isoform 2 activity stimulated by speeding up the rate of dissociation of ADP, *Biochemistry 43*, 13442−13451.
13. Hiromasa, Y., Hu, L., and Roche, T. E. (2006) Ligand-induced effects on pyruvate dehydrogenase kinase isoform 2, *J. Biol. Chem. 281*, 12568−12579.
14. Aicher, T. D., Anderson, R. C., Beberntiz, G. R., Coppola, G. M., Jewell, C. F., Knorr, D. C., Liu, C., Sperbeck, D. M., Brand, L. J., Strohschein, R. J., Gao, J., Vinluan, C. C., Shetty, S. S., Dragland, C., Kaplan, E. L., DelGrande, D., Islam, A., Liu, X., Lozito, R. J., Maniara, W. M., Walter, R. E., and Mann, W. R. (1999) (R)-3,3,3-Trifluoro-2-hydroxy-2-methylpropionamides are orally active inhibitors of pyruvate dehydrogenase kinase, *J. Med. Chem. 42*, 2741−2746.
15. Aicher, T. D., Anderson, R. C., Gao, J., Shetty, S. S., Coppola, G. M., Stanton, J. L., Knorr, D. C., Sperbeck, D. M., Brand, L. J., Winluan, C. C., Kaplan, E. L., Dragland, C. J., Tomaselli, H. C., Islam, A., Lozito, R. J., Liu, X., Maniara, W. M., Fillers, W. S., DelGrande, D., Walter, R. E., and Mann, W. R. (2000) Secondary amides of (R)-3,3,3-trifluoro-2-hydroxy-2-methylpropionic acid as inhibitors of pyruvate dehydrogenase kinase, *J. Med. Chem. 43*, 236−249.
16. Bebernitz, G. R., Aicher, T. D., Stanton, J. L., Gao, J., Shetty, S. S., Knorr, D. C., Strohschein, R. J., Tan, J., Brand, L. J., Liu, C., Wang, W. H., Vinluan, C. C., Kaplan, E. L., Drangland, C. J., DelGrande, D., Islam, A., Lozito, R. J., Liu, X., Maniara, W. M., and Mann, W. R. (2000) Anilides of (R)-trifluoro-2-hydroxy-2-methylpropionic acid as inhibitors of pyruvate dehydrogenase kinase, *J. Med. Chem. 43*, 2248−2257.
17. Morrell, J. A., Orme, J., Butlin, R. J., Roche, T. E., Mayers, R. M., and Kilgour, E. (2003) AZD7545 is a selective inhibitor of pyruvate dehydrogenase kinase 2, *Biochem. Soc. Trans. 31*, 1168−1170.
18. Mayers, R. M., Butlin, R. J., Kilgour, E., Leighton, B., Martin, D., Myatt, J., Orem, J. P., and Holloway, B. R. (2003) AZD7545, a novel inhibitor of PDHK2, activates PDH in vivo and improves blood glucose control in obese (fa/fa) Zucker rats, *Biochem. Soc. Trans. 31*, 1171−1173.
19. Mayers, R. M., Leighton, B., Butlin, R. J., and Kilgour, E. (2005) PDK kinase inhibitors: A novel therapy for type II diabetes, *Biochem. Soc. Trans. 33*, 367−370.
20. Ravindran, S., Radke, G. A., Guest, J. R., and Roche, T. E. (1996) Lipoyl domain-based mechanism for integrated feedback control of pyruvate dehydrogenase complex by enhancement of pyruvate dehydrogenase kinase activity, *J. Biol. Chem. 271*, 653−662.
21. Hiromasa, Y., and Roche, T. E. (2003) Facilitated interaction between the pyruvate dehydrogenase kinase isoform 2 and the dihydrolipoyl acetyltransferase, *J. Biol. Chem. 278*, 33681−33693.
22. Knoechel, T. R., Tucker, A. D., Robinson, C. M., Phillips, C., Taylor, W., Bungay, P. J., Kasten, S. A., Roche, T. E., and Brown, D. G. (2006) Regulatory roles of the N-terminal domain based on crystal structures of human pyruvate dehydrogenase kinase 2 containing physiological and synthetic ligands, *Biochemistry 45*, 402−415.
23. Steussy, N. C., Popov, K. M., Bowker-Kinley, M. M., Sloan, R. B., Harris, R. A., and Hamilton, J. A. (2001) Structure of pyruvate dehydrogenase kinase. Novel folding pattern for a serine protein kinase, *J. Biol. Chem. 276*, 37443−37450.
24. Kato, M., Chuang, J. L., Tso, S.-C., Wynn, R. M., and Chuang, D. T. (2005) Crystal structure of pyruvate dehydrogenase kinase 3 bound to lipoyl domain 2 of human pyruvate dehydrogenase complex, *EMBO J. 24*, 1763−1774.
25. Roche, T. E., and Reed, L. J. (1974) Monovalent Cation Requirement for ADP Inhibition of Pyruvate Dehydrogenase Kinase. *Biochem. Biophys. Res. Commun. 59*, 1341−1348.
26. Cate, R. L., and Roche, T. E. (1978) A unifying mechanism for stimulation of mammalian pyruvate dehydrogenase kinase activity by NADH, dihydrolipoamide, acetyl Coenzyme A, or pyruvate, *J. Biol. Chem. 253*, 496−503.
27. Pratt, M. L., and Roche, T. E. (1979) Mechanism of pyruvate inhibition of kidney pyruvate dehydrogenase$_a$ kinase and synergistic inhibition by pyruvate and ADP, *J. Biol. Chem. 254*, 7191−7196.
28. Machius, M., Chaung, J. L., Wynn, R. M., Tomchick, D. R., and Chuang, D. T. (2001) Structure of rat BCKD kinase: Nucleotide-induced domain communication in a mitochondrial protein kinase, *Proc. Natl. Acad. Sci. U.S.A. 98*, 11218−11223.
29. Hiromasa, Y., Fujisawa, T., Aso, Y., and Roche, T. E. (2004) Organization of the cores of the mammalian pyruvate dehydrogenase complex formed by E2 and E2 plus the E3-binding protein and capacities to bind the E1 and E3 components, *J. Biol. Chem. 279*, 6921−6933.
30. Blair, J. M. (1970) Magnesium, potassium, and the adenylate kinase equilibrium: Magnesium as a feedback signal from the adenine nucleotide pool, *Eur. J. Biochem. 13*, 384−390.
31. Portzehl, H., Caldwell, P. C., and Ruegg, J. C. (1964) The dependence of contraction and relaxation of muscle fibres from crab MAIA squinado on the internal concentration of free calcium ions, *Biochim. Biophys. Acta 79*, 581−591.
32. Lawlis, V. B., and Roche, T. E. (1980) Effect of micromolar Ca^{2+} on NADH inhibition of bovine kidney α-ketoglutarate dehydrogenase complex and possible role of Ca^{2+} in signal amplification, *Mol. Cell. Biochem. 32*, 147−152.
33. Turkan, A., Hiromasa, Y., and Roche, T. E. (2004) Formation of a complex of the catalytic subunit of pyruvate dehydrogenase phosphatase isoform 1 PDP1c and L2 domain forms a Ca^{2+}-binding site and captures PDP1c as a monomer, *Biochemistry 43*, 15073−15085.
34. Reinhart, G. D. (2004) Quantitative analysis and interpretation of allosteric behavior, *Methods Enzymol. 380*, 187−203.
35. Reinhart, G. D. (1988) Linked-function origins of cooperativity in a symmetrical dimer, *Biophys. Chem. 30*, 159−172.

36. Robertson, J. G., Barron, L. I., and Olson, M. S. (1989) Bovine heart pyruvate dehydrogenase kinase stimulated by monovalent ions, *J. Biol. Chem. 264*, 11626−11631.
37. Abrams, S. L., and Younathan, E. S. (1971) Modulation of the kinetic effect of phosphofructokinase by ammonium ions, *J. Biol. Chem. 246*, 2464−2467.
38. Nowak, T. (1976) Conformational changes required for pyruvate kinase activity as modulated by monovalent cations, *J. Biol. Chem. 251*, 73−78.
39. Wall, S. M. (2000) Impact of K^+ homeostasis on net acid secretion in rat terminal inner medullary collecting duct: Role of the Na,K-ATPase, *Am. J. Kidney Dis. 36*, 1079−1088.
40. Haussinger, D., Weiss, L., and Sies, H. (1975) Activation of pyruvate dehydrogenase during metabolism of ammonium ions in hemglobin-free perfused rat liver, *Eur. J. Biochem. 52*, 421−431.

BI701475F